Feature detection and scan area selection for 3D laser scanning sensors

Johannes Schlarp, Ernst Csencsics and Georg Schitter

***Abstract*— Due to the trend towards small lot sizes and fast changes of relevant product features in production processes, the demands for flexible measurement systems with high precision and throughput are constantly growing. By using optical scanning sensor systems, e.g. comprising a laser triangulation sensor and a fast steering mirror, the demands on speed and precision can be partially satisfied, leaving the flexibility of adapting to various measurement tasks to be solved. A common use-case is the need to measure a certain feature on a sample with a higher spatial resolution than the rest of the sample. By using machine vision such features can be detected automatically, enabling an automated adaptation of the scanning system to the measurement task. This work presents the combination of an optical scanning sensor system with an agglomerative clustering algorithm for detecting features and their dimensions. Based on the identified features, offset and scan amplitudes for high resolution rescans can be derived, resulting in a flexible metrology tool. Experimental results show that several individual features on a sample can be precisely detected and that an automatically parametrized rescan can significantly increase the lateral resolution of the acquired image.**

I. Introduction

Nowadays the fast changes of product features and small lot sizes of increasingly customized products, like in the PCB manufacturing or polymer processing, shown in Fig. 1, increase the need for flexible manufacturing devices [1]–[3]. At the same time the requirements on the product quality increase, such that also the demand for high resolution 3D measurement systems is increasing steadily [4]. To meet these requirements and obtain multidimensional metrology systems, most commonly optical point or line sensors are combined with external actuators like coordinate measurement machines [5], linear stages [6], [7] or industrial robots [8]. The achievable frame rate and spatial resolution of such component-based translational scanning systems is determined by the positioning bandwidth and the maximum force of the used actuators. In the case of optical sensors, it is, however, also possible to manipulate only the optical path instead of displacing the entire sensor system. Since the moving mass of such a compact rotational scanner can be low compared to a classical translational scanning system, measurement times can be decreased [9]. Recently such a scanning system, which consists of a laser triangulation sensor and a fast steering mirror (FSM), has been proposed [10].

A common case in measurement applications is that certain areas on a sample need to be imaged with higher spatial resolution than the rest of the sample [11]. This enables for example to check if the specified tolerances or dimensions of a feature of interest are satisfied [12]. One approach to achieve the required resolution in the specified area is to scan the entire sample with the required resolution. However, given physical system limitations, the achievable frame rate can be significantly decreased by this approach. Considering a constant scan speed the measurement time would increase directly proportional with the increase in resolution. By scanning just the sub-area containing the feature of interest with the required resolution, this drawback can be avoided. This, however, requires an adaptation of the measurement system to the particular measurement task. Such an adaptation can typically be realized by either programming or teaching the features of an individual product to the measurement system, which is in times of short production cycles and quickly changing products, however, inefficient and resource-intensive [12], [13].

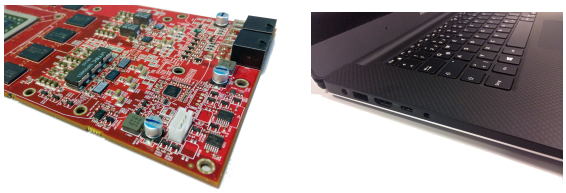

(a) (b)

Fig. 1. The increasing number of customized products in (a) PCB manufacturing or (b) polymer processing leads to fast changes of relevant product features, such that flexible manufacturing devices are required.

Using machine vision, the individual features on a sample can be recognized and rescanned adaptively, without the need to statically tailor the measurement task to the specific product sample [14]. Since the features have striking characteristics like gradients in height or color, the interest points of various features can be detect with point detection algorithms (e.g. harris point detection) [15]. The assignment of individual interest points to one feature is, however, difficult [16]. This issue can be solved by employing clustering algorithms, with k-means or agglomerative clustering algorithms being most commonly used for multiple feature detection [17]. From the result of the clustering algorithm, the center point as well as lateral dimensions of each feature can be derived. Since the scan trajectories of the optical scanning system are freely selectable, they can be adapted to the required resolution and the derived dimensions of the individual feature.

The contribution of this paper is the automated adaptation

The authors are with the Christian Doppler Laboratory for Precision Engineering for Automated In-Line Metrology at the Automation and Control Institute (ACIN), Vienna University of Technology, 1040 Vienna, Austria. Corresponding author: schlarp@acin.tuwien.ac.at

Post-print version of the article: J. Schlarp, E. Csencsics, and G. Schitter, "Feature detection and scan area selection for 3D laser scanning sensors", *IEEE/ASME International Conference on Advanced Intelligent Mechatronics (AIM)*, pp. 280–285, 2018. DOI: 10.1109/AIM.2018.8452235

of a novel optical scanning system for 3D metrology with a clustering algorithm, to detected and rescan features without any information about the sample, leading to a flexible metrology system. In Section II the experimental setup of the scanning system is presented. To calculate the surface profile from the measured data, the geometrical relations are derived in Section III. The approach to detect the individual features is presented in Section IV, followed by the experimental results shown in Section V. The paper is concluded in Section VI.

II. Scanning Laser Triangulation Sensor System

A. System hardware

The experimental setup of the optical scanning system, shown in Fig. 2, consists of a laser triangulation sensor (Type: ILD 2300-100, Micro-Epsilon GmbH, Germany), with a measurement range of 100 mm and a FSM (Type: OIM102, Optics In Motion LLC, Long Beach, USA) with an aperture size of two inches. To acquire 3D images both optical paths of the laser sensor are manipulated by the FSM. By tilting the mirror surface around the x or yz'-axis, the position of the laser spot on the sample is manipulated along the y or x-axis, respectively. Both, the illumination and the reflection path are redirected by the mirror surface, such that the basic measurement geometry is not affected from the perspective of the triangulation sensor. As a result, the scanning system satisfies the Scheimpflug condition, leading to a sharp projection of the diffusely reflected point from the sample onto the detector [11].

B. Scan trajectory

To scan a two-dimensional area of interest an appropriate scan trajectory is required. Raster scan trajectories are commonly employed scan patterns [18]. They are generated by driving the system axes of the FSM with one slow and one fast triangular signal, resulting in a uniform scan speed and spatial resolution. To track the triangular signal at least the first seven harmonics of the fundamental frequency need to be covered by the system bandwidth [19]. A high spatial and temporal resolution requires a high system bandwidth, which is challenging as it is typically limited by structural modes of the system [19].

Recently also Lissajous trajectories have been applied to precision scanning systems, such as atomic force microscopes [20]. To generate these trajectories each system axis is driven with a sinusoidal signal of a single frequency, with the frequencies determining the spatial and temporal resolution. Due to their multi-resolution property an early overview of the entire scan are is generated and is continuously refined with evolving scan time. The simplicity of the driving signals further enables a tailoring of the scanner dynamics, such that with resonance carefully tuned to the drive frequencies the energy consumption can be significantly decreased [21]. Due to these advantages, especially the multi-resolution property, a Lissajous trajectory is used for the scanning triangulation sensor system.

For choosing the two drive frequencies two conditions need to be considered: (i) the maximum achievable frequency, at which the entire actuation range is still available, is limited to 52 Hz by the maximum actuator current of the FSM and (ii) to reduce the crosstalk between the two system axes the frequencies need to be well separated. According to these conditions the two driving frequencies 52 Hz and 27 Hz are chosen, such that a framerate of 1 frame/s and a spatial resolution of 0.058 (with respect to unity image size) is achieved.

C. Motion control

Since the controller only needs to track the driving frequency of the controlled system axis and reject the driving frequency of the other system axis in the case of the applied Lissajous trajectory, a dual tone controller can be used [21]. The loop gain of the system with dual tone controllers shows high gain values only at the two drive frequencies and quickly decreasing gains towards lower and higher frequencies, which reduces sensor noise feedback [20]. The controllers are implemented on a dSpace platform (Type: DS1202, dSPACE GmbH, Germany) with a sampling rate of 20 kHz. The measured distance of the triangulation sensor as well as the position of the FSM are also acquired and processed using the dSpace platform. Fig. 2 also shows manual linear stages that are used to align the sensor, with respect to the FSM.

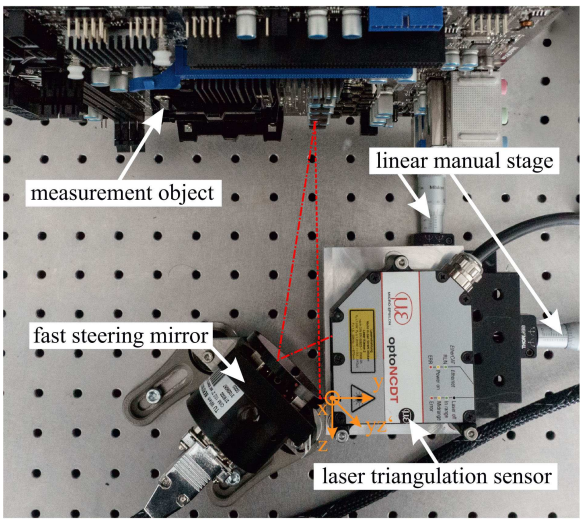

Fig. 2. Experimental setup of the scanning laser triangulation sensor. Both optical paths of the laser sensor are manipulated by the FSM. To align the sensor two manual linear stages are used.

III. Geometrical Relations for Data Reconstruction

The measured quantities of the scanning system consist of the distance z_{meas} which is acquired by the triangulation sensor and the angular positions $\Delta\varphi$, $\Delta\vartheta$ of the FSM. Since the surface profile of the sample is described by the absolute

Post-print version of the article: J. Schlarp, E. Csencsics, and G. Schitter, "Feature detection and scan area selection for 3D laser scanning sensors", *IEEE/ASME International Conference on Advanced Intelligent Mechatronics (AIM)*, pp. 280–285, 2018. DOI: 10.1109/AIM.2018.8452235

values x_l, y_l and z_l, the profile cannot be directly obtained from the measured quantities. By deriving the geometrical relations the surface profile can be calculated from the measured values. The calculation of these relations is based on the setup geometry of the scanning system, shown in Fig. 3.

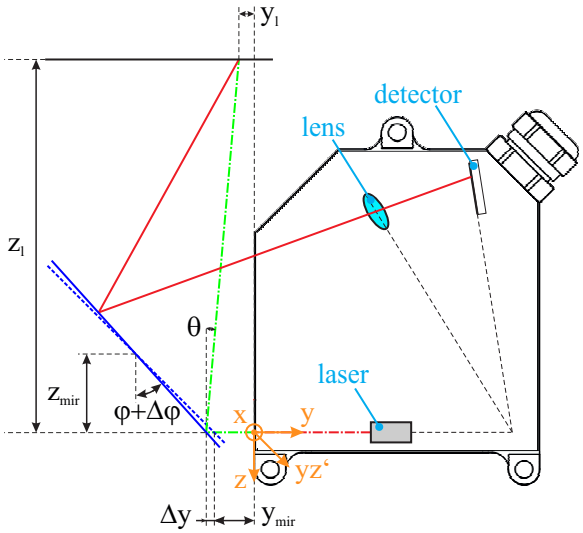

Fig. 3. Schematic setup of the scanning system. As the illumination path does not hit the center of the mirror, an additional lateral displacement Δy needs to be considered. The total length of the dashed-dotted line (green) represents the measured distance z_{meas}.

As depicted in the setup geometry, the illuminating laser beam does not hit the center of the FSM, such that there is an additional translational displacement of the mirror surface, and the measurement spot on the sample, in the y-direction. This additional displacement can be considered by

$$\Delta y = z_{mir}[\tan(\varphi) - \tan(\varphi - \Delta\varphi)], \tag{1}$$

with φ the orientation of the FSM and z_{mir} its position in z-direction. To determine the position at which the emitted laser beam hits the sample, the two angles of reflection from the FSM in the yz and xz-plane are required. By using the law of reflection the angles can be calculated to

$$\theta = \frac{\pi}{2} - 2\varphi - 2\Delta\varphi \tag{2a}$$
$$\gamma = (2\Delta\vartheta) \cdot \cos(\varphi + \Delta\varphi), \tag{2b}$$

with $\Delta\varphi$ and $\Delta\vartheta$ the angular positions of the mirror around the x and yz'-axis, respectively. By using trigonometric functions the geometrical relations of the optical scanning system can be derived to

$$x_l = [z_{meas} - y_{mir} - \Delta y]\cos(\theta)\sin(\gamma) \tag{3a}$$
$$y_l = [z_{meas} - y_{mir} - \Delta y]\sin(\theta)\cos(\gamma) - y_{mir} - \Delta y \tag{3b}$$
$$z_l = -[z_{meas} - y_{mir} - \Delta y]\cos(\theta)\cos(\gamma), \tag{3c}$$

with y_{mir} the position of the FSM in y-direction and z_{meas} the measured distance (dash-dotted line, green). The parameters of the scanning systems are selected to maximize the achievable lateral scan range. This is achieved by choosing the angular orientation φ to $45°$ and positioning the FSM as close as possible to sensor. To avoid a collision between sensor and FSM the distances y_{mir} and z_{mir} are set to 10 mm and 16.5 mm, respectively. Since the actuation range of the FSM is $\pm 1.5°$, a lateral scan range of about ± 8 mm is obtained.

IV. Feature Detection

To detect the individual features on the sample, most commonly k-means or agglomerative clustering algorithms are used [15], [16]. For the k-means algorithm the number of clusters is predefined, such that the algorithm must be adapted if the number of features on the sample changes [17]. However, for the agglomerative clustering algorithm only the maximum distance between two points is set in advance. Since the dimensions of the features generally do not change within a product group, this parameter can be kept constant even if the number of features changes.

The agglomerative clustering algorithm initially assumes that each data point is a cluster. Subsequently the two closest clusters are merged to a new set which consists of both previous clusters and the previous clusters are removed. This process is repeated until the distance between the two closest clusters is larger than a predefined maximum distance [16]. Thereby, each data point in an image is assigned to a cluster and each cluster represents a feature on the sample [15].

The calculation time of the clustering algorithm is strongly determined by the number of measured points [15]. By sub-sampling the entire acquired image, the computational time can be reduced without significantly influencing the result [22]. A more efficient approach is to already employ the multi-resolution property of the Lissajous trajectories and acquire only a low-resolution image of the sample for the feature detection. This approach reduces not only the computational time but also the measurement time.

After the clustering algorithm has converged, the required scan area as well as the center point of each feature can be determined. Each cluster is examined for the minimal and maximal position in x and y-direction and the resulting scan area is enlarged by a factor of 1.2, in order to assure that the complete feature is rescanned. By rearranging Eqns. 3 to obtain $\Delta\vartheta$ and $\Delta\varphi$, the required offsets and scan amplitudes in x and y-direction for each feature are determined. Besides the scan amplitudes, the spot diameter of the used triangulation sensor represents the ultimate limitation for the highest lateral resolution that can be achieved. As a result, it must be considered that the resolution of the determined scan trajectory is larger than the spot diameter, as otherwise only the measurement time is increased.

V. Experimental Results

To validate the automated feature detection and trajectory adaptation of the scanning triangulation sensor system a PCB

Post-print version of the article: J. Schlarp, E. Csencsics, and G. Schitter, "Feature detection and scan area selection for 3D laser scanning sensors", *IEEE/ASME International Conference on Advanced Intelligent Mechatronics (AIM)*, pp. 280–285, 2018. DOI: 10.1109/AIM.2018.8452235

sample containing a transistor and two SMD resistors is used (shown in Fig. 4(a)). Initially an overview measurement of the entire sample, shown in Fig. 4(b)), is acquired with the optical scanning system and the already described geometrical relations.

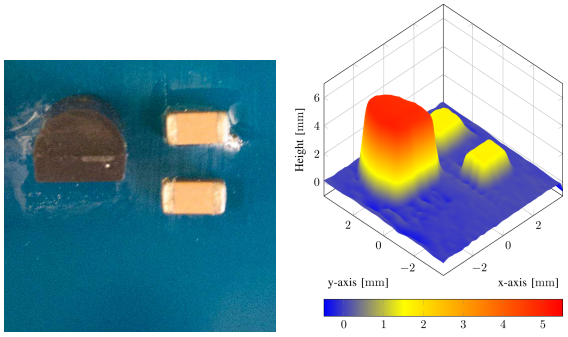

(a) Measurement object (b) Surface profile of the sample

Fig. 4. Measurement sample. (a) shows an image and (b) the measurement result of the overview scan.

The agglomerative clustering algorithm is applied to the acquired image to obtain center points and dimensions of the various features. To detect the individual features the maximum distance between the clusters is set to 0.3 mm, which is appropriate since each dimension of the different components is larger then 1 mm. In Fig. 5 the result of the clustering algorithm is depicted. Each detected cluster,

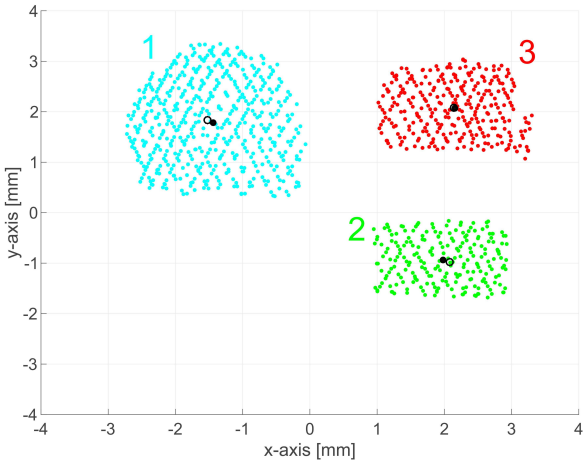

Fig. 5. Result of the clustering algorithm. All three features (one transistor, two SMD resistors) were detected separately. Also the center of each feature is shown (black dot).

equaling a separate feature, is displayed in a different color together with its calculated center of gravity (black). Compared to the image of the sample in Fig. 4(a) the clustering, results in objects of similar shape, position and orientation. The position (center of gravity) and lateral dimensions of the detected features are listed in Table II. With the lateral dimension and Eqn. 3 the required offset and scan amplitudes for each feature are determined. The effective maximum lateral resolution for the rescan of two selected components with the chosen scan trajectory are listed in Table I. The resolution in the z-direction is determined by the laser triangulation sensor, leading to a constant resolution for the different scans.

TABLE I
RESOLUTION OF THE DIFFERENT SCANS.

	x [μm]	y [μm]	z [μm]
Sample	483	548	30
First Feature	225	226	30
Second Feature	159	128	30

To reduce number of measurement points and thus the computational time of the clustering algorithm, a sub-sampled measurement of the entire scan area can be used. Due to the multi-resolution property of Lissajous trajectories the measurement can be stopped after a fraction of the entire frame time, resulting in a lower resolution measurement of the entire scan area. For evaluation an overview image of the entire sample, acquired in 0.25 s (one quarter of the scan time), is fed to the clustering algorithm. This reduces the computational time from 1.48 s to 0.237 s, which equals a reduction by a factor of 6.2. The calculated centers of gravity of all clusters are shown in Fig. 5 (black circles) and listed in Table II. The maximum shift of the center points compared to the full-resolution image is 0.11 mm. Since the scan area is enlarged by a factor of 1.2 and the smallest detected lateral dimension is 1.6 mm, a rescan with the obtained parameters still captures the entire feature.

TABLE II
CALCULATED DIMENSIONS AND CENTER POINTS OF THE INDIVIDUAL FEATURES.

	Feature 1	Feature 2	Feature 3
x_{min}	-2.72 mm	0.95 mm	1.02 mm
x_{max}	-0.07 mm	2.93 mm	3.3 mm
x_{center}	-1.44 mm	1.98 mm	2.15 mm
$x_{center,T_{mess}/4}$	-1.53 mm	2.08 mm	2.14 mm
y_{min}	0.33 mm	-1.68 mm	1.07 mm
y_{max}	3.34 mm	-0.17 mm	3.03 mm
y_{center}	1.78 mm	-0.94 mm	2.07 mm
$y_{center,T_{mess}/4}$	1.84 mm	-0.98 mm	2.08 mm

The scan trajectories of the overview scan and the rescan of the SMD resistor are compared in Fig. 6. It can be seen that the achievable resolution in x and y-direction in case of the rescan can be improved by a factor of 3.

In Fig. 7 the results of the rescan for the transistor (a) and one SMD resistor (b) are shown. Compared to the overview scan shown in Fig. 4(b) the increased level of detail is

Post-print version of the article: J. Schlarp, E. Csencsics, and G. Schitter, "Feature detection and scan area selection for 3D laser scanning sensors", *IEEE/ASME International Conference on Advanced Intelligent Mechatronics (AIM)*, pp. 280–285, 2018. DOI: 10.1109/AIM.2018.8452235

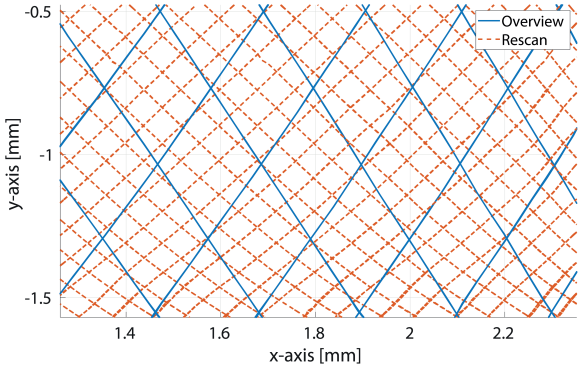

Fig. 6. The scan trajectories for the overview scan (solid, blue) and the rescan of the SMD resistor (dashed, red) are shown. By rescanning this feature with the adapted scan trajectory, the achievable resolution can be significantly increased.

apparent in the resulting high-resolution images. Even the soldering contacts on the SMD resistor are observable (magenta, circle). If a CAD-model of the sample is available, an overlay could be used to determined whether the dimensions and positions of the individual components comply with the specifications.

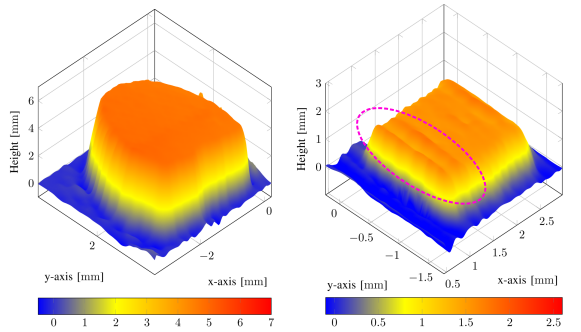

(a) Transistor (b) SMD resistor

Fig. 7. The measured surface profile of two detected features (transisor, SMD resistor) are shown. Even the soldering contacts on the SMD resistor are observable (magenta, circle).

In summary it was shown that with the proposed scanning triangulation sensor system features on a sample can automatically be detected and rescanned with a higher resolution, enabling a flexible adaptation of the measurement system to an arbitrary task.

VI. Conclusion

In this paper an optical scanning system is extended by an agglomerative clustering algorithm, to automatically detect features on a sample and rescan them with a higher resolution. By determining the geometrical relations of the scanning system, the surface profile of the sample can be reconstructed from the distance measured with the sensor and the measured mirror position. Due to the multi-resolution property of Lissajous trajectories, the scan process for an overview scan of the entire sample can already be terminated after a fraction of the entire scan time without loosing critical information. This reduces the measurement time and number of measurement points, such that also the computational time of the clustering algorithm can be decreased without significantly altering the result. Since the result of the algorithm only depends on the chosen maximum distance between the clusters, the algorithm can be easily adapted to the measurement application. The experimental results show, that each feature is detected individually and can be rescanned automatically with a tuned amplitude and offset, resulting in detailed scan with higher lateral resolution.

Acknowledgment

The financial support by the Austrian Federal Ministry for Digital, Business and Enterprise, and the National Foundation for Research, Technology and Development, as well as MICRO-EPSILON MESSTECHNIK GmbH & Co. KG and ATENSOR Engineering and Technology Systems GmbH is gratefully acknowledged.

References

[1] R. Schmitt and F. Moenning, "Ensure success with inline-metrology," *XVIII IMEKO world congress Metrology for a Sustainable Development*, 2006.
[2] H. Schwenke, U. Neuschaefer-Rube, T. Pfeifer, and H. Kunzmann, "Optical methods for dimensional metrology in production engineering," *CIRP Annals-Manufacturing Technology*, vol. 51, no. 2, pp. 685–699, 2002.
[3] G. Sansoni, M. Trebeschi, and F. Docchio, "State-of-the-art and applications of 3d imaging sensors in industry, cultural heritage, medicine, and criminal investigation," *Sensors*, vol. 9, no. 1, pp. 568–601, 2009.
[4] F. Blais, "Review of 20 years of range sensor development," *Journal of Electronic Imaging*, vol. 13, no. 1, 2004.
[5] T. Pfeifer, *Koordinatenmeßtechnik für die Qualitätssicherung: Grundlagen-Technologien-Anwendungen-Erfahrungen*. Springer-Verlag, 2013.
[6] M. Levoy, K. Pulli, B. Curless, S. Rusinkiewicz, D. Koller, L. Pereira, M. Ginzton, S. Anderson, J. Davis, J. Ginsberg, J. Shade, and D. Fulk, "The digital michelangelo project: 3d scanning of large statues," *Proceedings of the 27th annual conference on Computer graphics and interactive techniques*, pp. 131–144, 2000.
[7] F. J. Brosed, J. J. Aguilar, D. Guilloma, and J. Santolaria, "3d geometrical inspection of complex geometry parts using a novel laser triangulation sensor and a robot," *Sensors*, vol. 11, no. 1, pp. 90–110, 2010.
[8] H. Kunzmann, T. Pfeifer, R. Schmitt, H. Schwenke, and A. Weckenmann, "Productive metrology - adding value to manufacture," *CIRP Annals-Manufacturing Technology*, vol. 54, no. 2, pp. 155–168, 2005.
[9] C. Yu, X. Chen, and J. Xi, "Modeling and calibration of a novel one-mirror galvanometric laser scanner," *Sensors*, vol. 17, no. 1, p. 164, 2017.
[10] J. Schlarp, E. Csencsics, and G. Schitter, "Optical scanning of a laser triangulation sensor for 3d imaging," *IEEE Transactions on Instrumentation and Measurement*, 2018, submitted.
[11] A. Donges and R. Noll, *Laser measurement technology*. Atlanta: Springer, 2015.
[12] C. P. Keferstein and W. Dutschke, *Fertigungsmesstechnik*. Wiesbaden: Springer Vieweg, 2010.
[13] A. Weckenmann, H. Eitzert, M. Garmer, and H. Weber, "Functionality-oriented evaluation and sampling strategy in coordinate metrology," *Precision engineering*, vol. 17, no. 4, pp. 244–252, 1995.
[14] G. B. Coleman and H. C. Andrews, "Image segmentation by clustering," *Proceedings of the IEEE*, vol. 67, no. 5, pp. 773–785, 1979.
[15] R. Szeliski, *Computer vision: algorithms and applications*. Springer Science & Business Media, 2010.

Post-print version of the article: J. Schlarp, E. Csencsics, and G. Schitter, "Feature detection and scan area selection for 3D laser scanning sensors", *IEEE/ASME International Conference on Advanced Intelligent Mechatronics (AIM)*, pp. 280–285, 2018. DOI: 10.1109/AIM.2018.8452235

[16] W. E. Snyder and H. Qi, *Machine Vision*. Cambridge University Press, 2010.
[17] C. Steger, M. Ulrich, and C. Wiedemann, *Machine vision algorithms and applications*. John Wiley & Sons, 2018.
[18] L. R. Hedding, "Fast steering mirror design and performance for stabilization and single axis scanning," in *Acquisition, Tracking, and Pointing IV*, vol. 1304. International Society for Optics and Photonics, 1990, p. 14.
[19] J. A. Fleming and G. A. Wills, "Optimal periodic trajectories for band-limited systems," *IEEE Transactions on Control Systems Technology*, vol. 17, no. 3, pp. 552–562, 2009.
[20] T. Tuma, J. Lygeros, V. Kartik, A. Sebastian, and A. Pantazi, "High-speed multiresolution scanning probe microscopy based on lissajous scan trajectories," *Nanotechnology*, vol. 23, no. 18, p. 185501, 2012.
[21] E. Csencsics and G. Schitter, "System design and control of a resonant fast steering mirror for lissajous-based scanning," *IEEE Transactions on Mechatronics*, vol. 22, no. 5, pp. 1963–1972, 2017.
[22] P. S. Bradley, U. M. Fayyad, and C. Reina, "Scaling clustering algorithms to large databases," *KDD*, pp. 9–15, 1998.

Post-print version of the article: J. Schlarp, E. Csencsics, and G. Schitter, "Feature detection and scan area selection for 3D laser scanning sensors", *IEEE/ASME International Conference on Advanced Intelligent Mechatronics (AIM)*, pp. 280–285, 2018. DOI: 10.1109/AIM.2018.8452235